ISSN 1068-3372, Journal of Contemporary Physics (Armenian Academy of Sciences), 2022, Vol. 57, No. 1, pp. 91–97. © Allerton Press, Inc., 2022.
Russian Text © The Author(s), 2022, published in Izvestiya Natsional'noi Akademii Nauk Armenii, Fizika, 2022, Vol. 57, No. 1, pp. 131–140.

Rocking Curves of X-Ray Asymmetrical Laue Diffraction in a Crystal with the Third-Order Nonlinear Response

M. K. Balyan*

Yerevan State University, Yerevan, Armenia

**e-mail: mbalyan@ysu.am*

Received September 8, 2021; revised October 27, 2021; accepted November 14, 2021

Abstract—The X-ray Laue asymmetrical diffraction in a perfect crystal with a plane entrance surface is considered taking into account the third-order nonlinear response of a crystal. Using the exact solutions, the rocking curve dependence on the angular departure from the exact Bragg direction and the intensity of the incident wave is investigated. The dependence of rocking curves on the asymmetry degree of diffraction geometry is studied. The obtained results can be used in the preparation of X-ray beams with the given parameters and for object investigations as well.

Keywords: X-rays, asymmetrical diffraction, third-order nonlinearity, rocking curves

DOI: 10.3103/S1068337222010078

1. INTRODUCTION

The transmission and reflection coefficients of a dynamically diffracted X-ray plane wave on the output surface of the crystal depend on the parameter of the deviation from the Bragg angle, the thickness of the crystal plate, and the degree of asymmetry of the diffraction geometry. As for the case of beams of high intensity, such as beams of synchrotron sources of X-ray radiation of the third generation or the X-ray lasers on free electrons, it is necessary to take into account the nonlinear term of the third order in the polarizability of the crystal. Then the intensity of the incident beam also becomes one of the parameters of the problem. Bragg diffraction is used both for studying objects and obtaining beams with specified parameters. The latter means the preparation of beams with the required degree of monochromaticity, collimation, or the preparation of a focused beam. But in the case of beams with high intensity, it is necessary to investigate the Bragg nonlinear diffraction. One of the important features of Bragg nonlinear diffraction is the rocking curves, that is the dependence of the transmission and reflection coefficients on the deviation from the Bragg angle [1, 2], and, in the nonlinear case, also on the intensity of the incident wave at a fixed thickness and angle of asymmetry. The basic equations of dynamic X-ray diffraction in a crystal with a cubic nonlinear response to an external electromagnetic field were obtained in [3]. For the case of symmetric reflection, the exact Bragg solution was found in [4]. In the Laue case, the exact solution taking into account the deviation from the Bragg angle as well as the asymmetry of diffraction was found in [5]. These solutions made it possible to study the nonlinear diffraction and its basic laws in a crystal. It turned out to be that the pendulum effect also takes place in the nonlinear case. An analytical expression was found for the extinction length. The equations of dynamic nonlinear diffraction can also be solved numerically. In [6], a third-order nonlinear dynamic diffraction was numerically investigated for an incident beam with a limited wavefront. The study of nonlinear diffraction of the third order of X-ray pulses was carried out in [7].

At present, the theoretical and experimental studies of second and third-order nonlinear X-ray effects are also being carried out. The second-order non-linear effect is the parametric down-conversion. The essence is that because of the nonlinear response of the crystal the initial photon decays into two photons with a lower frequency so that the frequency of the original photon is equal to the sum of the frequencies of the generated photons. In the region of X-ray, this effect was first predicted in [8]. The effect was experimentally observed and studied in [9–19] using both laboratory and synchrotron X-ray sources. Another X-ray nonlinear effect of the second order, the generation of the second harmonic, was studied theoretically in [20] and experimentally observed in [21]. The nonlinear Compton effect was studied experimentally in [22], and theoretically in [23]. The X-ray cubic-nonlinear single-wave diffraction was theoretically studied in [24], the nonlinear mixing of four waves in [25], and the X-ray two-photon absorption in [26].

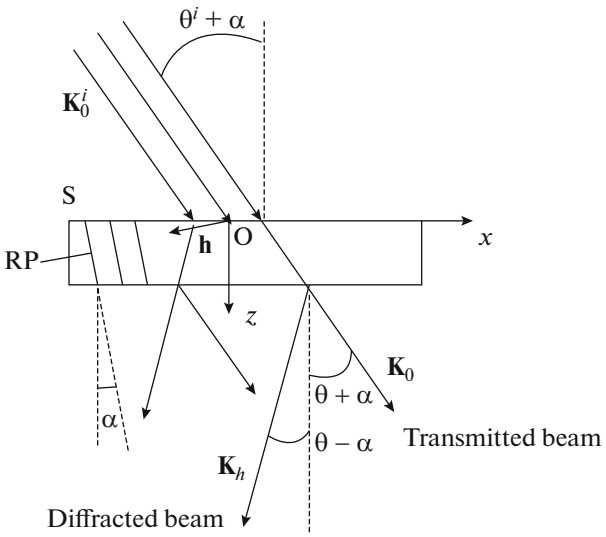

Fig. 1. Scheme of asymmetric Laue diffraction: $\mathbf{K}_0^i$ is the mean wave vector of the incident wave, θ^i is the angle between the wave vector and the reflecting planes, θ is the Bragg angle, α is the angle between the reflecting planes RP and the internal normal to the input surface S, Oxz is the coordinate system in the diffraction plane, the Oy axis is directed perpendicular to the diffraction plane according to the law of the right-hand coordinate system, $\mathbf{K}_0$ and $\mathbf{K}_h = \mathbf{K}_0 + \mathbf{h}$ are the wave vectors of the transmitted and diffracted waves that satisfy the exact Bragg condition, and $\mathbf{h}$ is the diffraction vector perpendicular to the reflecting planes.

Below, we study the rocking curves in the case of cubically nonlinear asymmetric Laue diffraction in a perfect crystal, based on the exact solutions obtained in [5]. The rocking curves are investigated both as a function of the deviation from the Bragg angle and on the intensity of the incident wave.

2. BASIC FORMULAS

The scheme of asymmetric Laue diffraction is shown in Fig. 1. The reflecting planes RP are deflected from the position perpendicular to the input surface by an asymmetry angle, which in the case of transmission diffraction varies within $|\alpha| < \pi/2 - \theta$. This angle is considered to be positive if the deviation from the position perpendicular to the input surface occurs counterclockwise, and is negative when deflected in the opposite direction. A plane X-ray wave σ-polarized with amplitude E^i is incident on the crystal at a grazing angle θ^i to the reflecting planes close to the Bragg angle. Two strong waves, transmitted and diffracted, with amplitudes E_0 and E_h, appear in the crystal. It is believed that the thickness of the crystal is rather small and absorption can be neglected, that is $\mu z < 1$, where μ is the absorption coefficient of the crystal. It is also believed that the intensity of the incident wave can be so high that it is necessary to take into account the cubic nonlinear term in the expression of the crystal polarizability. In addition, it is assumed that reflection with the diffraction vector $2\mathbf{h}$ is forbidden, that is the corresponding Fourier coefficients of both linear and nonlinear polarizability are equal to zero.

As mentioned in the Introduction, the exact solutions were found in [5]. We will investigate the transmission $T(z) = |E_0|^2/|E^i|^2$ and reflection coefficients $R(z) = \gamma_h |E_h|^2/(\gamma_0 |E^i|^2)$ based on these exact solutions. The transmission and reflection coefficients depend on the sign of Q (the definition of Q is just below). It is necessary to distinguish between the following cases: $Q > 0$, $Q < 0$, $Q = 0$ and $q_1 < 0$, $Q = 0$ and $q_1 > 0$. The following notation is adopted here [5]:

$$Q = q_1^2/4 + q_2^3/27, \tag{1}$$

$q_1 = 2(a/3)^3 - ab_1/3 + c$, $q_2 = -a^2/3 + b_1$, $a = \beta_2/\beta_1$, $b_1 = \beta_3/\beta_1$, and $c = \beta_4/\beta_1$. Moreover, $\beta_1 = (\alpha_4^2 - \alpha_2)$, $\beta_2 = I_1(\alpha_2 - \alpha_4^2) + 2\alpha_3\alpha_4 - \alpha_1$, $\beta_3 = 1 + I_1(\alpha_1 - 2\alpha_3\alpha_4) + \alpha_3^2$, and $\beta_4 = -I_1\alpha_3^2$. Coefficients α_i included here are defined as $\alpha_1 = (1-b)[2 + I_1(1-b)/(1-I_1)]/(1-I_1)$,

$\alpha_2 = -(1-b)^2/(1-I_1)^2$, $\alpha_3 = -b^{1/2}\sin 2\theta[\Delta\theta - \chi_0(1-b)[1 - I_1(1+b)/2]/(2b\sin 2\theta)]/[|\chi_h|(1-I_1)]$, $\alpha_4 = |\chi_0|(1-4b+b^2)/[4b^{1/2}|\chi_h|(1-I_1)]$. These expressions include $b = \gamma_0/\gamma_h$, which is the coefficient of asymmetry, $\gamma_{0,h} = \cos(\theta \pm \alpha)$ are the direction cosines of the wave vector of the incident wave to the direction of the internal normal to the input surface of the crystal, θ is the Bragg angle, $\chi_{0,h}$ are the Fourier coefficients of crystal polarizability for the zero reciprocal lattice vector and the reflection vector $\mathbf{h}$, $y = y_0/(1-I_1)$, $y_0 = b^{1/2}\sin 2\theta[\Delta\theta - \chi_0(1-b)/(2b\sin 2\theta)]/|\chi_h|$ is the parameter of deviation from the Bragg condition, $\Delta\theta = \theta^i - \theta$ is the angle of deviation from the Bragg condition, $I_1 = I/I_{\max}$ is the critical intensity normalized, $I_{\max}$ is the incident wave intensity $I = \left|E_0^i\right|^2$, E_0^i is the constant incident wave amplitude, $I_{\max} \approx 2.1\times10^{25}$ V^2/m^2 is the intensity at which the corresponding intensity of the X-ray wave $E_{\max} = \sqrt{I_{\max}} \approx 4.6\times10^{12}$ V/m is equal to the strength of the atomic nucleus at a distance of the Bohr radius (the expression for this quantity see in [5] and the references given there). The transmission and reflection coefficients depend on the angle of deviation from the exact Bragg angle, on the intensity of the incident beam, and the angle made up by the reflecting planes and the normal to the entrance surface of the crystal. Below, we investigate the transmission and reflection coefficients depending on the deflection parameter and on the intensity of the incident wave for a fixed crystal thickness and various values of the asymmetry angle of the reflecting planes.

3. ROCKING CURVES OF CUBIC NONLINEAR ASYMMETRIC LAUE DIFFRACTION

We investigate the rocking curves for Si(111) reflection with a radiation wavelength $\lambda = 0.71$ Å, the incident wave is plane and σ-polarized (the electric field vector is perpendicular to the diffraction plane). In this case, the reflection of Si(222) is forbidden and the above formulas can be applied for thicknesses for which absorption can be neglected.

3.1. Rocking Curves Versus Angular Deviation from the Bragg Condition

First, let us consider the case $\alpha = -60°$ ($b = 1.49$). To compare the linear and nonlinear cases in Fig. 2a for the intensity $I_1 = 10^{-5}$, which corresponds to the linear case, the transmission and reflection rocking curves are shown depending on the angular deviation from the exact Bragg angle $\Delta\theta$ (on the graph, the angles are given in arc seconds, this interval of angles corresponds to the interval of the parameter y_0, $[-2, 2]$), and $Q > 0$. The thickness was selected as $z = 2\Lambda_{NL} \approx 40.6$ μm with the deviation parameter $y_0 = 0$. Here, Λ_{NL} is the extinction length of the nonlinear case for $Q > 0$ [5]. This quantity, in contrast to the linear case, also substantially depends on the intensity of the incident wave. Because the intensity is so low that the linear case is realized, the extinction length of the nonlinear case coincides with the extinction length of the linear case [1, 2]

$$\Lambda_L == \frac{\lambda(\gamma_0\gamma_h)^{1/2}}{|\chi_h|\sqrt{1+y_0^2}}, \tag{2}$$

which depends on the deviation parameter and does not depend on the intensity. Note that for the selected thickness $\mu z = 0.06$. Because the thickness is chosen equal to two extinction lengths, then maximum transmission coefficient and minimum reflection coefficient corresponding to the angular deviation $\Delta\theta = \chi_0(1-b)/(2b\sin 2\theta)$ (at this point $y_0 = 0$), correspond to the value $y_0 = 0$. This is well known in linear theory as refraction correction for the Bragg condition to be fulfilled [1, 2]. Let us see how the rocking curves change with increasing intensity. Figures 2b and 2c show the rocking curves for intensities $I_1 = 0.2$ and $I_1 = 0.4$, for the depths $z = 2\Lambda_{NL}(y_0 = 0, I_1 = 0.2) \approx 54.9$ μm and $z = 2\Lambda_{NL}(y_0 = 0, I_1 = 0.4) \approx 71.8$ μm, respectively. Note that $\mu z = 0.08$ and $\mu z = 0.1$. For these parameter values $Q > 0$. The extinction depths are computed using the corresponding formula in [5]. As can be seen from these figures, the widths of the main transmission maxima and the main reflection minima narrow, and the coordinates of their centers decrease. This shift of coordinates is explained by the fact that as shown in [5], the role of the deviation parameter, taking into account the intensity, is played by

$$\alpha_3 = -b^{1/2}\sin 2\theta[\Delta\theta - \chi_0(1-b)[1 - I_1(1+b)/2]/(2b\sin 2\theta)]/[|\chi_h|(1-I_1)]$$

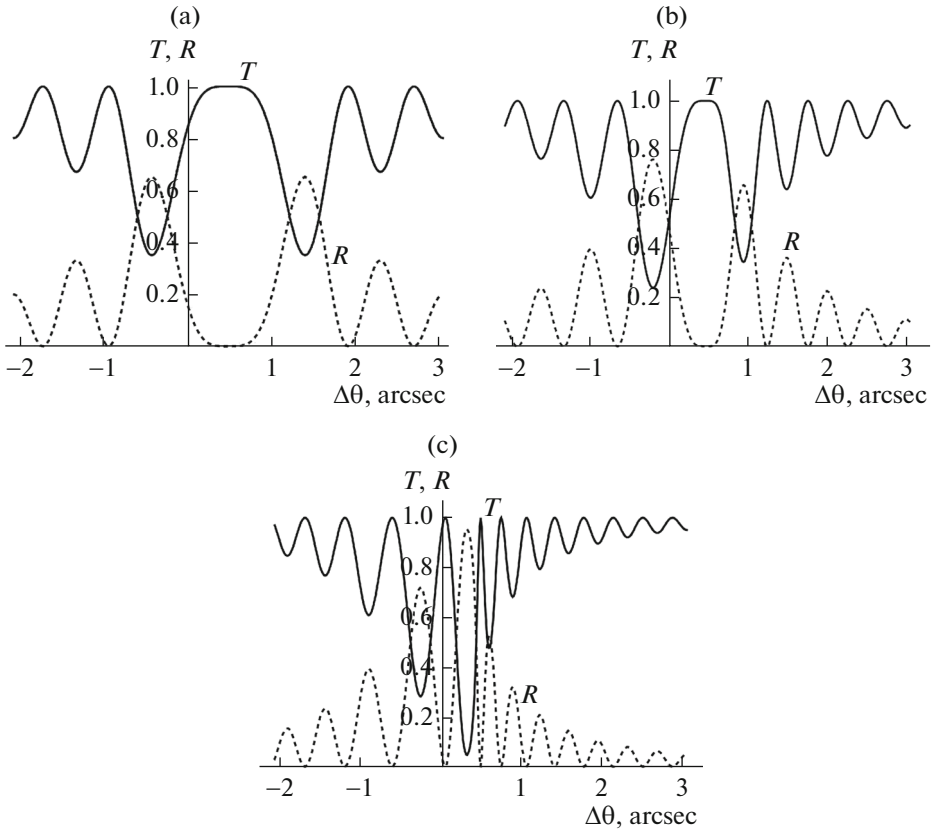

Fig. 2. Rocking curves for case $\alpha = -60°$, solid curves are the transmission coefficient, dashed line is the reflection coefficient. (a) Linear case, (b) $I_1 = 0.2$, and (c) $I_1 = 0.4$.

(for the definition of α_3 see explanations after formula (1)) so that the main maximum and minimum are shifted to the point Fig. 3. $\Delta\theta = \chi_0(1-b)[1 - I_1(1+b)/2]/(2b\sin 2\theta)$, corresponding to the value $\alpha_3 = 0$. It is clear that the new position of the main maximas and minimas no longer corresponds to $y_0 = 0$. These figures also show the appearance of asymmetry of the main maximas and minimas, as well as periods of oscillations on both sides of the main maximas and minimas.

The rocking curves depending on the deflection of the parameter y_0 are represented in Fig. 3 for the case $\alpha = -60°$ ($b = 0.67$). The dependences are given on the angle of deflection, and the segment of the deflection parameter [–2, 2]corresponds to the shown segment of the angles $\Delta\theta$. Figure 3a shows the rocking curve corresponding to the linear theory: the intensity of the incident wave $I_1 = 10^{-5}$. The depth is taken to be equal to $z = 40.6\,\mu$m, which corresponds to two extinction lengths of the linear case (2) for the deviation parameter. This depth in the linear theory does not differ from the corresponding value for the case $\alpha = -60°$. Because $b < 1$, then, due to refraction, the main maximum of the transmitted beam and the main minimum of the diffracted beam is displaced in the opposite direction, in comparison with the case $b > 1$ shown in Fig. 2a. This point corresponds to the parameter $y_0 = 0$ and, in addition, the widths of the main maximum and minimum are greater than in the case $\alpha = -60°$. These are well-known facts in linear theory [1, 2]. Now let us continue to monitor the change in the rocking curves by increasing the intensity of the incident wave. Figures 3b and 3c show the rocking curves for the intensity values $I_1 = 0.2$ and $I_1 = 0.4$. As can be seen from these figures, the widths of the main highs and lows decrease again, and the coordinates of the main peaks and main lows increase, in contrast to the case $b > 1$. This is again explained by the fact that, in the nonlinear case, the coordinates of the main peaks and minima are determined as $\Delta\theta = \chi_0(1-b)[1 - I_1(1+b)/2]/(2b\sin 2\theta)$. In these examples $Q > 0$. The depths are taken equal to 48.5 and 59.6 μm, which correspond to the two extinction lengths of the nonlinear case for the value

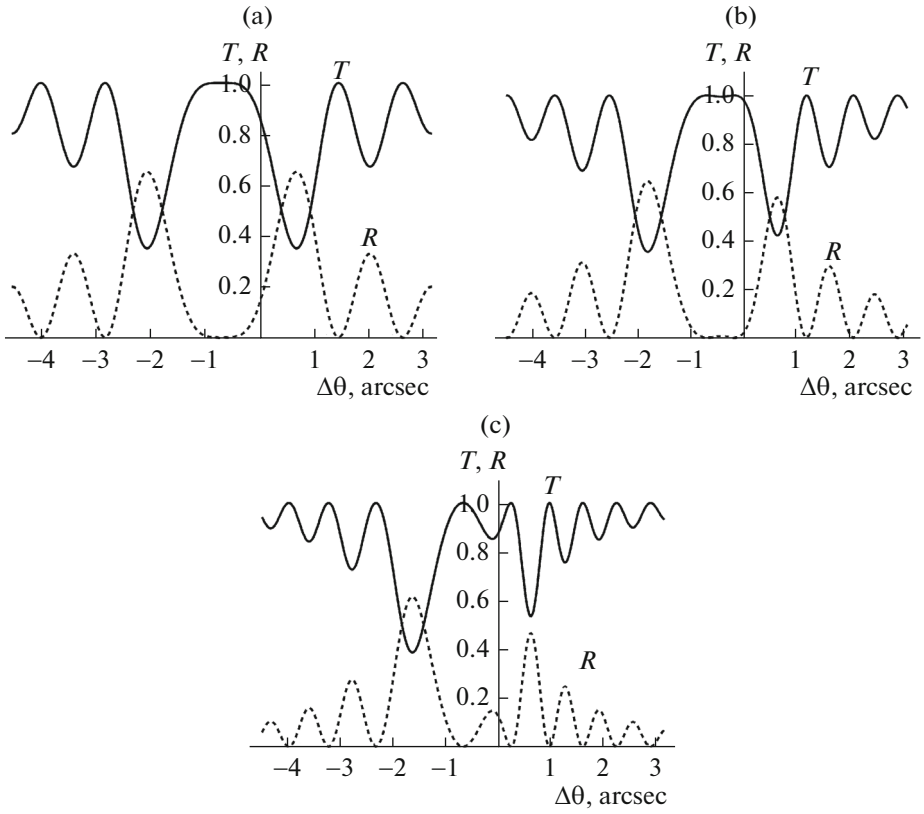

Fig. 3. Rocking curves for the case $\alpha = 60°$, solid curves are transmission coefficient, dashed line is reflection coefficient. (a) Linear case, (b) $I_1 = 0.2$, and (c) $I_1 = 0.4$.

$y_0 = 0$. At these depths, the absorption is negligible and the above formulas for the transmission and reflection coefficients can be applied.

3.2. Rocking Curves Dependent on the Intensity

In contrast to the linear case, in the nonlinear case, the transmission and reflection coefficients also depend on the intensity of the incident wave. In this section, based on the formulas for the transmission and reflection coefficients, we will investigate the rocking curves depending on the intensity of the incident wave.

Let us consider the case $\alpha = -60°$. We will consider the transmission and reflection coefficients at depths $z = 2\Lambda_L(y_0)$. In all cases, the absorption is negligible, and the expressions for the transmission and reflection coefficients given in [5] can be applied. At $y_0 = -2$, the quantity $Q > 0$ for all values of intensities [5]. Applying the appropriate formulas [5] and taking $z = 2\Lambda_L(y_0 = -2) = 18.2$ μm, we find the dependence of the transmission and reflection coefficients on the intensity. These dependencies are shown in Fig. 4. We recall again that in the linear case the rocking curves are independent of the intensity.

Let us give a separate example of when Q can be either more or less than zero. We take $\alpha = -60°$, $y_0 = -0.5$, the depth $z = 2\Lambda_L(y_0 = -0.5) = 36.3$ μm. Sign dependence graph Q is represented in Fig. 5. It can be seen that starting from the value $I_1 = 0.67$, the sign Q changes from positive to negative. Therefore, in the region before this value, the rocking curves are determined by the corresponding formula $Q > 0$, and starting from this intensity value, the rocking curves are determined by the formula to $Q < 0$ [5]. Figure 6 shows the rocking curves versus intensity over the entire range of variation. As one can see, the behavior of the rocking curves changes starting from the intensity value $I_1 = 0.67$. In this region, the energy is mainly concentrated in the transmitted beam.

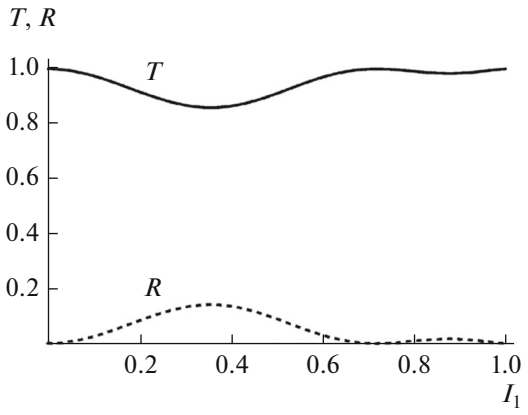

Fig. 4. Rocking curves versus intensity for the case $\alpha = -60°$, $y_0 = -2$; the solid curve is the transmitted wave curve, the dotted line is the rocking curve of the diffracted wave.

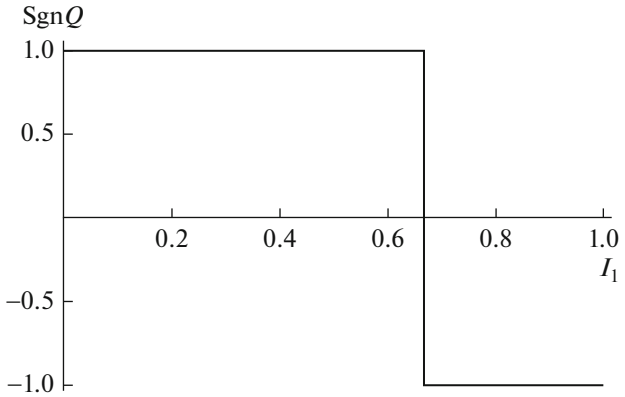

Fig. 5. The dependence of the sign of the function on the intensity for $\alpha = -60°$ and $y_0 = -0.5$.

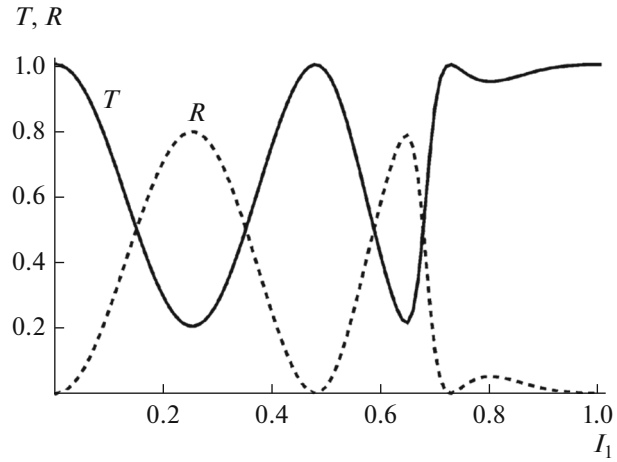

Fig. 6. Rocking curves versus intensity for the case $\alpha = -60°$, $y_0 = -2$; the solid curve is the transmitted wave curve, the dotted line is the rocking curve of the diffracted wave.

4. CONCLUSION

Rocking curves are one of the important and practically applicable characteristics of dynamic X-ray diffraction. If in the region of low intensities, where the linear theory of polarizability is applicable, these curves are well studied both theoretically and experimentally, then the same cannot be said for high-intensity beams, for which nonlinear terms in the polarizability of the crystal are important. Currently, high-intensity sources of X-ray radiation, the synchrotrons, and X-ray free-electron lasers, have stimulated interest in the theoretical and experimental study of nonlinear X-ray effects. In this work, the rocking curves of cubic nonlinear Bragg asymmetric diffraction in the transmission geometry are investigated. The previously obtained exact solutions made it possible to plot the rocking curves in the entire range of variation of independent parameters, such as the parameter of deviation from the Bragg condition and the intensity of the incident wave. The rocking curves are obtained for various angles of asymmetry.

The results obtained can be applied in further theoretical and experimental studies of nonlinear X-ray diffraction, as well as for obtaining beams with specified parameters or for studying objects.

REFERENCES

1. Authier, A., *Dynamical Theory of X-ray Diffraction*, Oxford: University Press, 2001.
2. Pinsker, Z.G., *Rentgenovskaya kristallooptika* (X-ray Crystal Optics), Moscow: Nauka, 1982.
3. Balyan, M.K., *Crystallogr. Rep.*, 2015, vol. 60, p. 993.
4. Balyan, M.K., *J. Synchrotron Rad.*, 2015, vol. 22, p. 1410.
5. Balyan, M.K., *Physica scripta*, 2021, vol. 96, p. 125006.
6. Balyan, M.K., *J. Contemp. Phys.*, 2016, vol. 51, p. 391.
7. Balyan, M.K., *J. Synchrotron Rad.*, 2016, vol. 23, p. 919.
8. Freund, I. and Levine, B.F., *Phys. Rev. Lett.*, 1969, vol. 23, p. 854.
9. Eisenberger, P. and McCall, S.L., *Phys. Rev. Lett.*, 1971, vol. 26, p. 684.
10. Adams, B., Fernandez, P., Lee, W-K., Materlik, G., Mills, D., and Novikov, D., *J. Synchrotron Rad.*, 2000, vol. 7, p. 81.
11. Yoda, Y.T., Suzuki, T., Zhang, X-W., Hirano, K., and Kikuta, S., *J. Synchrotron Rad.*, 1998, vol. 5, p. 980.
12. Shwartz, S., Coffe, R.N., Feldkamp, J.M., Feng, Y., Hastings, J.B., Yin, G.Y., and Harris, S.E., *Phys. Rev. Lett.*, 2012, vol. 109, p. 013602.
13. Schori, A., Bömer, C., Borodin, D., Collins, S., Detlefs, B., Morett, M., Yudovich, S., and Shwartz, S., *Phys. Rev. Lett.*, 2017, vol. 119, p. 253902.
14. Danino, H. and Freund, I., *Phys. Rev. Lett.*, 1981, vol. 46, p. 1127.
15. Tamasaku, K. and Ishikawa, T., *Phys. Rev. Lett.*, 2007, vol. 98, p. 244801.
16. Tamasaku, K. and Ishikawa, T., *Acta Cryst.*, 2007, vol. A63, p. 437.
17. Borodin, D., Levy, S., and Shwartz, S., *Appl. Phys. Lett.*, 2017, vol. 110, p. 131101.
18. Barbiellini, B., Joly, Y., and Tamasaku, K., *Phys. Rev. B*, 2015, vol. 92, p. 155119.
19. Borodin, D., Schori, A., Rueff, J.-P., Ablett, J.M., and Shwartz, S., *Phys. Rev. Lett.*, 2019, vol. 122, p. 023902.
20. Nazarkin, A., Podorov, S., Uschmann, I., Förster, E., and Sauerbrei, R., *Phys. Rev. A*, 2003, vol. 67, p. 041804.
21. Shwartz, S., Fuchs, M., Hastings, J.B., Inubushi, N., Ishikawa, T., Katayama, T., Reis, D.A., Sato, T., Tono, K. Yabashi, M., Yudovich, S., and Harris. S.E., *Phys. Rev. Lett.*, 2014, vol. 112, p. 163901.
22. Fuchs, M., Trigo, M., Chen, J., Ghimire, Sh., Shwartz, Sh., Kozina, M., Jiang, M., Henighan, T., Bray, C., Ndabashimiye, G., Bucksbaum, Ph., Feng, Y., Herrmann, S., Carini, G., Pines, J., Hart, Ph., Kenney, Ch., Guillet, S., Boutet, S., Williams, G.J., Messerschmidt, M., Seibert, M.M., Moeller, S., Hastings, J.B., and Reis, D., *Nature Physics*, 2015, vol. 11, p. 964.
23. Krebs, D., Reis, D., and Santra, R., *Phys. Rev. A*, 2019, vol. 99, p. 022120.
24. Conti, C., Fratallocchi, A., Ruocco, G., and Sette, F., *Opt. Express*, 2008, vol. 16, p. 8324.
25. Tanaka, S. and Mukamel, S., *Phys. Rev. Lett.*, 2002, vol. 89, p. 043001.
26. Tamasaku, K., Shigemasa, E., Inubushi, Y., Katayama, T., Sawada, K., Yumoto, H., Ohashi, H., Mimura, H., Yabashi, M., Yamauchi, K., and Ishikawa, T., *Nature Photon Lett.*, 2014, vol. 8, p. 313.

Translated by V. Musakhanyan